Electronic Supplementary Material (ESI) for Chemical Communications.

Short-wavelength ultraviolet dosimeters based on DNA nanostructure-modified graphene field-effect transistors

Zhaolin Ai,[ab§] Liqian Wang,[ab§] Qianying Guo,[ab] Derong Kong,[ab] Yungen Wu,[ab] Yunqi Liu[b] and Dacheng Wei*[a]

** Corresponding authors. E-mail: weidc@fudan.edu.cn.*

§ Zhaolin Ai and Liqian Wang contributed equally to this work.

[a] State Key Laboratory of Molecular Engineering of Polymers, Department of Macromolecular Science, Fudan University, Shanghai 200433, China.

[b] Institute of Molecular Materials and Devices, Fudan University, Shanghai 200433, China.

1 Experimental section

1.1 Materials

All designed staple strands were prepared and purified by Sangon (Shanghai, China). M13mp18 circular ss-DNA was purchased from New England Biolabs (Beverly, Massachusetts, USA). SYBR Safe, agarose, magnesium chloride solution and gel loading buffer were purchased from Thermal Fisher (Waltham, Massachusetts, USA). 1-pyrenebutanoic acid succinimidyl ester (PASE) was purchased from Sigma Aldrich (St. Louis, Missouri, USA). All the aqueous solutions were prepared using distilled water produced by the Milli-Q Integral 3 ultrapure water polishing system of Merck (Darmstadt, Germany) with a resistivity of 18 MΩ cm^{-1}.

1.2 Synthesis of DNA structures

The rectangular DNA origami was assembled in 1× TAE-Mg^{2+} buffer solution (40 mM Tris-acetate, 1 mM EDTA, and 12.5 mM magnesium chloride, pH 8.0–8.4) by the reported annealing program using the SimpliAmp thermal cycler of Thermo Fisher.[1] DNA tetrahedron was synthesized in 1× TM buffer solution (50 mM Tris, 8 mM magnesium chloride, pH 7.0–7.4). The annealing program starts at 95 °C for 5 min, then immediately cools to 4 °C.[2] The synthesized DNA origami was purified by Amicon Ultra (100K) centrifugal filters of Merck Millipore (Darmstadt, Germany) to remove the excess short strands of DNA.

1.3 UV exposure

The UVC emission was produced by the Philips UVC lamp (15W), and centred at 254 nm through the 254 nm optical filter. The radiation intensity of the UVC lamp was 1.67 W m^{-2} after filtering, measured by the S120VC standard photodiode power sensor of Thorlabs (Newton, New Jersey, USA). The samples were exposed to UVC for variable times (0, 0.167, 0.333, 0.5, 1, 2, 3, 4, 5, 10, 30, 60, and 120 min), corresponding to the doses of 0, 0.0167, 0.0333, 0.05, 0.1, 0.2, 0.3, 0.4, 0.5, 1, 3, 6 and 12 kJ m^{-2}, respectively. The UVA emission of 365 nm was produced by multi-

UV lamp and the radiation intensity of UVA lamp was 2.78 W m^{-2}, measured by the S120VC standard photodiode power sensor of Thorlabs. Then the samples were exposed to UVA for variable times (0, 1, 4, and 12 h), corresponding to the doses of 0, 10, 40 and 120 kJ m^{-2}, respectively.

1.4 Characterization

Gel electrophoresis experiments were performed in 0.8% agarose gel for DNA origami and in 2% agarose gel for DNA tetrahedron with 1× TAE-Mg^{2+} buffer solution and pre-strain with 0.01% SYBR Safe. 8 μL of UV-treated sample was mixed with 2 μL of 6× loading buffer and then loaded in each well. The electrophoresis ran at 95 V for 60 min in ice-water mixture, then the gels were imaged by a XR+ gel imaging system of Bio-rad (Hercules, California, USA). AFM images of DNA nanostructures on mica and on graphene surface were obtained by using the Dimension Fast Scan AFM system of Bruker (Billerica, Massachusetts, USA) under ScanAsyst-Air mode with ScanAsyst-Air tips of Bruker. For sample preparation on mica, 5 μL of each DNA origami samples was pipetted to mica surface and incubated for 20 min at room temperature. Then each sample was rinsed with 100 μL of deionized water and blown dry with nitrogen gently and immediately. Field emission scanning electron microscopy (FESEM) images of DNA nanostructures on graphene surface were obtained by using Gemini SEM500 of Zeiss (Oberkochen, Germany).

1.5 Fabrication of the dosimeters

Cr and Au with thicknesses of 5 nm and 50 nm are patterned on the Si/SiO_2 substrates by photolithography as the electrodes, which were deposited by the Covap vacuum evaporation system of Angstrom Engineering (Ontario, Canada). The monolayer graphene grown by chemical vapor deposition (CVD) was transferred onto the patterned substrates to fabricate a FET device. The sensing regions were defined by patterning graphene channels via photolithography and oxygen plasma etching techniques. The devices were submerged in 5 mM PASE and acetone solution for 12 hours at room temperature to assemble a monolayer of PASE on graphene through

π–π stacking, then it was rinsed with water and ethanol alternately for several times to remove extra PASE. The modified graphene devices were immersed in DNA nanostructure buffer solution by PDMS well for 24 hours to immobilize DNA nanostructures on graphene channels, followed by rinsing with water gently to remove extra DNA nanostructures. The incubation concentration of ss-DNA, ds-DNA, DNA tetrahedron and DNA origami is 2 μM, 1 μM, 10 nM and 1 μM.

1.6 Device measurement

The electrical signals were measured by the B1500A semiconductor analyzer of Keysight (Santa Clara, California, USA). Ag/AgCl reference electrode was used as the liquid gate electrode. V_{lg} was set between −0.8 and +0.8V versus Ag/AgCl and the V_{ds} was set to 50 mV in which no electrochemical reaction occurs on the graphene or electrodes. The current variation signals were normalized as $\Delta I/I_0 = (I_0–I_{ds})/I_0$, where I_{ds} is the real-time drain-source current and I_0 is the current of the initial dosimeters. The error bars were calculated from test results of 5 different devices via the mean and standard deviation model.

2 Supplementary Notes

2.1 Sequences of staple strands (5’ to 3’)

2.1.1 tetrahedron

ACATTCCTAAGTCTGAAACATTACAGCTTGCTACACGAGAAGAGCCGCCATAGTA

NH_2-C_6-
TATCACCAGGCAGTTGACAGTGTAGCAAGCTGTAATAGATGCGAGGGTCCAATAC

NH_2-C_6-TCAACTGCCTGGTGATAAAACGACACTACGTGGGAATCTACTATGGCGGCTCTTC

NH_2-C_6-TTCAGACTTAGGAATGTGCTTCCCACGTAGTGTCGTTTGTATTGGACCCTCGCAT

2.1.2 DNA Origami

Modified DNA strands:

AAACAGTTGATGGCTTAGAGCTTATTTAAATATTTT-C_6NH_2

TCAGAAGCCTCCAACAGGTCAGGATCTGCGAATTTT- C_6NH_2

ATTATTTAACCCAGCTACAATTTTCAAGAACGTTTT- C_6NH_2

CTTTACAGTTAGCGAACCTCCCGACGTAGGAATTTT- C_6NH_2

CTTAAACATCAGCTTGCTTTCGAGAAACAGTTTTTT- C_6NH_2

GAATAAGGACGTAACAAAGCTGCTGACGGAAATTTT- C_6NH_2

TTTTAATTGCCCGAAAGACTTCAATTCCAGAGTTTT- C_6NH_2

AGACAGTCATTCAAAAGGGTGAGATATCATATTTTT- C_6NH_2

TTCGCCATTGCCGGAAACCAGGCAAACAGTACTTTT- C_6NH_2

CCGAAATCCGAAAATCCTGTTTGAAATACCGATTTT- C_6NH_2

2.3 ss-DNA and ds-DNA

ss-DNA:

NH_2-C_6-CCATACCCTTTCCACATACCGCAGAGGC

ds-DNA:

NH_2-C_6-CCATACCCTTTCCACATACCGCAGAGGC

GCCTCTGCGGTATGTGGAAAGGGTATGG

2.2 Calculation of LoDs

Response curves of the UVC dosimeters follow the 'S-shaped curves' which are typical dose response curves. The linear standard curves are fitted in the linear detection range to calculate the LoDs of the UVC dosimeters. The noises are taken from the difference of the highest and lowest responses in real-time I_{ds} versus time curves, as shown in Fig. S10. Noises plus three times are taken as the noise levels and the LoDs are calculated from the intersection of the noise levels and the linear standard curves, as shown in Fig. S11. The confidence of the calculation method is higher than 99.99% in a normal distribution model, for the noise levels are set as higher than the standard deviations of real-time I_{ds} plus ten times. The noise levels of UVC dosimeters working in buffer solution and in air are 0.0736% and 0.1111% respectively. The calculated LoDs are 0.0051 kJ m^{-2} and 0.0061 kJ m^{-2} in UVC dosimeters modified with DNA tetrahedron and DNA origami working in buffer solution respectively, while the LoDs of UVC dosimeters working in air are 0.0058 kJ m^{-2} and 0.0065 kJ m^{-2} respectively.

2.3 Density and equivalent charge of PASE and DNA nanostructures

Application of a liquid-gated g-FET leads to the formation of electrical double layers (EDLs) at a polarizable electrode/electrolyte interface[3]. The EDLs at liquid-graphene interfaces can be considered as insulating layers. The total gate capacitance (C_{tot}) of a g-FET is made of the EDL capacitance C_{liq} and the quantum capacitance of graphene C_Q in series with:

$$\frac{1}{C_{tot}} = \frac{1}{C_{liq}} + \frac{1}{C_Q} = \frac{1}{c_{liq}S_{liq}} + \frac{1}{c_Q S_Q} \#(1)$$

Here, c_{tot}, c_{liq} and c_Q are the capacitances per unit area. S_{tot}, S_{liq} and S_Q are the contact areas which can be considered as the channel areas. Each channel area S is equal to 30×60 μm^2. c_Q is graphene quantum capacitance per unit area of ~20 mF m^{-2}.[4,5] The EDL capacitance c_{iq} is estimated as ~96 mF m^{-2}.[3] The total gate capacitance per unit area (c_{tot}) of g-FET is calculated as ~17 mF m^{-2}.

The charge change ΔQ and Dirac point shift ΔV_{Dirac} occur when the PASE and DNA nanostructures are anchored on the graphene channel surface:

$$\Delta V_{Dirac} = \Delta Q\left(\frac{1}{C_{liq}} + \frac{1}{C_Q}\right) \#(2)$$

$$\Delta Q = q\, S\, n \#(3)$$

Here, n is the modification density, q is the equivalent charge per molecule of modification. According to the equation (1), (2) and (3), ΔV_{Dirac} is equal to 60 q n V m^2 C^{-1}, which is proportional to the equivalent charge per molecule q and density n. The ΔV_{Dirac} versus bare g-FETs of the devices modified by PASE and DNA nanostructures is shown in Fig. S9c.

The density of PASE n_{PASE} can be quantitatively evaluated from the comparison between graphene modified with PASE and PASE solution. According to Lambert-Beer's law, it is assumed that molar absorption coefficient (ε) is constant both in membrane and in solution:

$$n_{PASE} = c_{PASE}\, l_{PASE} = \frac{A_{PASE}}{\varepsilon} \#(4)$$

Here, n_{PASE}, c_{PASE}, l_{PASE} and A_{PASE} are the modification density of PASE, concentration of PASE solution, thickness and absorbance of graphene modified with PASE, respectively. ε is calculated as ~4100 m^2 mol^{-1} and n_{PASE} is estimated as ~2.2×10^{18} m^{-2}. The density of DNA nanostructures is counted from FESEM images (five images, 1×1 μm^2) and AFM images (five images, 1×1 μm^2), examples are shown in Fig. S4, Fig. S2b and Fig. S3a. The density of DNA origami n_{ori} and the density of DNA tetrahedron n_{tetra}

138 can be estimated as 10±4 μm^{-2} and 85±11 μm^{-2} respectively. Thus, the equivalent charge per PASE q_{PASE}

139 is ~8.7×10^{-22} C. And the equivalent charge per DNA origami q_{ori} and the equivalent charge per DNA

140 tetrahedron q_{tetra} can be calculated as ~6.2×10^{-17} C and ~8.0×10^{-18} C, which is equal to the charge carried

141 by 385 electrons and 50 electrons respectively.

3 Supplementary Figures

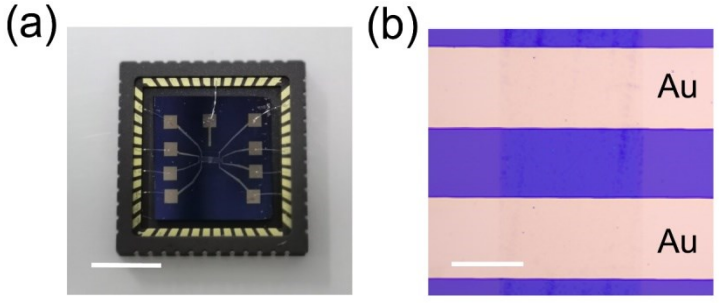

Fig. S1. (a) Photograph and (b) optical microscope image of the UVC dosimeters. Scale bars: (a) 500 μm and (b) 40 μm.

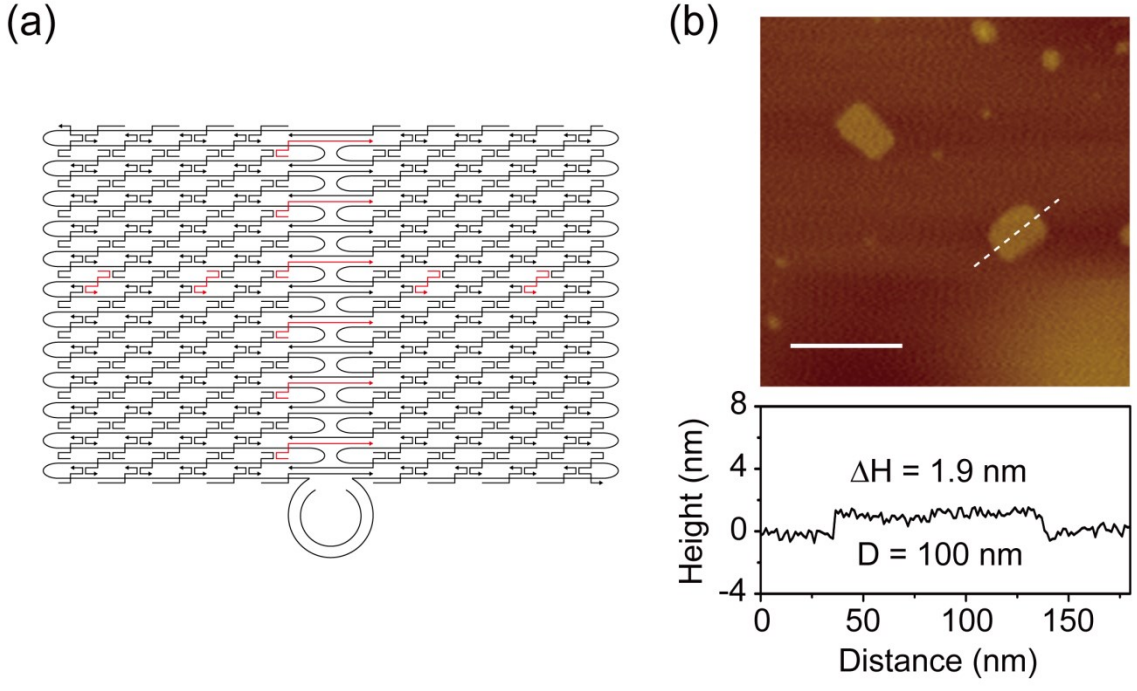

Fig. S2. (a) Design diagram of the rectangular DNA origami.[1] Red lines represent staple strands which are modified with amino groups. (b) AFM image of the DNA origami on mica. Scale bar is 200 nm.

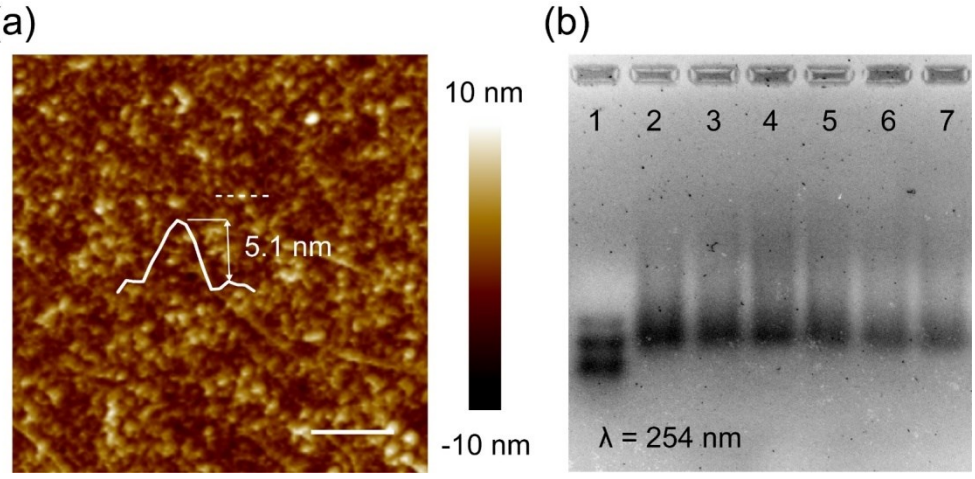

Fig. S3. (a) AFM image of the DNA tetrahedron on graphene surface. Scale bar is 200 nm. (b) AGE characterizations of DNA tetrahedron at various UVC doses. Lanes 1–7: DNA marker, 0, 0.1, 0.3, 0.5, 1, and 3 kJ m^{-2} doses, respectively. The image colour is inverted to display more clearly.

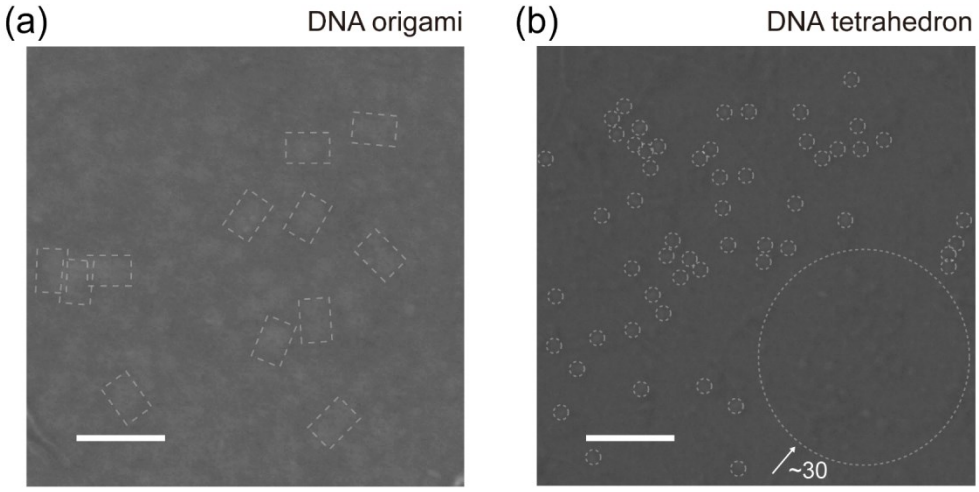

Fig. S4. (a) FESEM image of graphene immobilized with DNA origami. (b) FESEM image of graphene immobilized with DNA tetrahedron. Some of the nanostructures are marked with white dotted line and the scale bars are 200 nm.

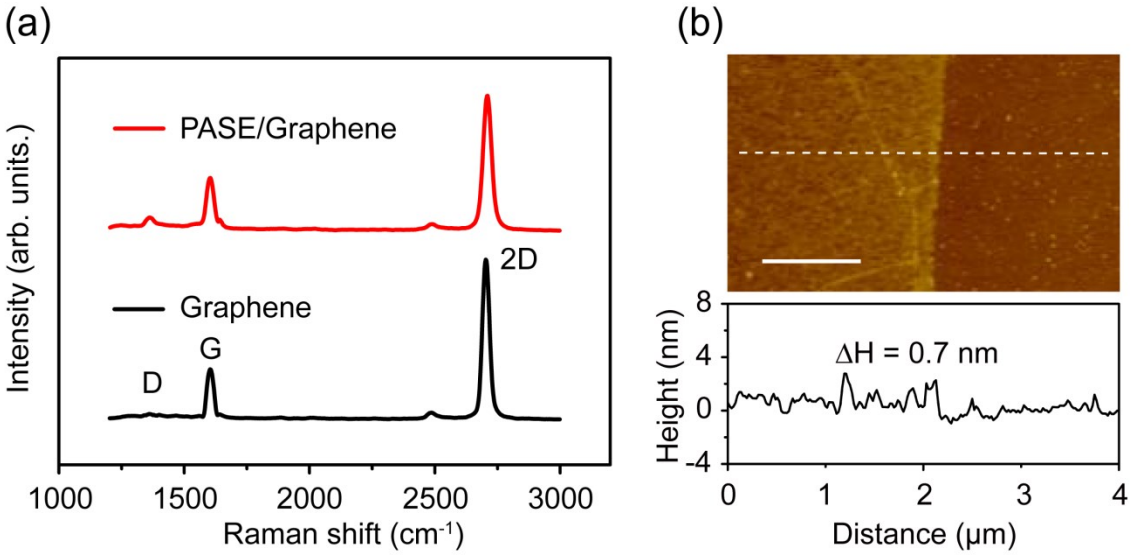

158

159 **Fig. S5.** (a) Raman spectra of graphene and PASE modified graphene. The tiny D peak and a high intensity
160 ratio of the 2D peak with the G peak in Raman spectra of graphene indicate high quality and monolayer
161 nature of the CVD grown samples. (b) AFM image of the monolayer graphene. Scale bar is 1 μm.

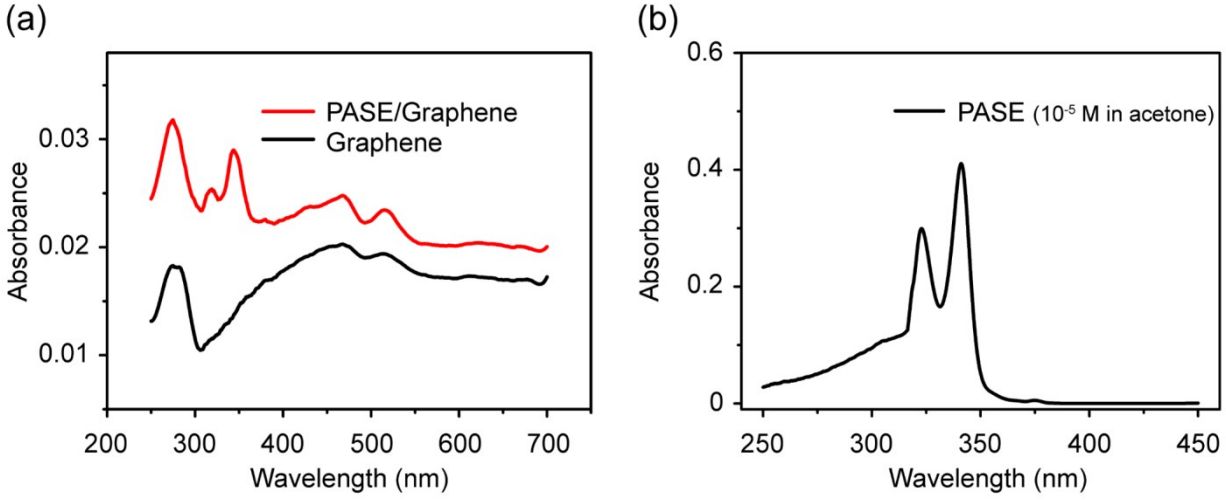

162

163 **Fig. S6.** (a) UV-vis absorption spectra of graphene and PASE modified graphene. (b) UV-vis absorption
164 spectrum of 10^{-5} M PASE in acetone.

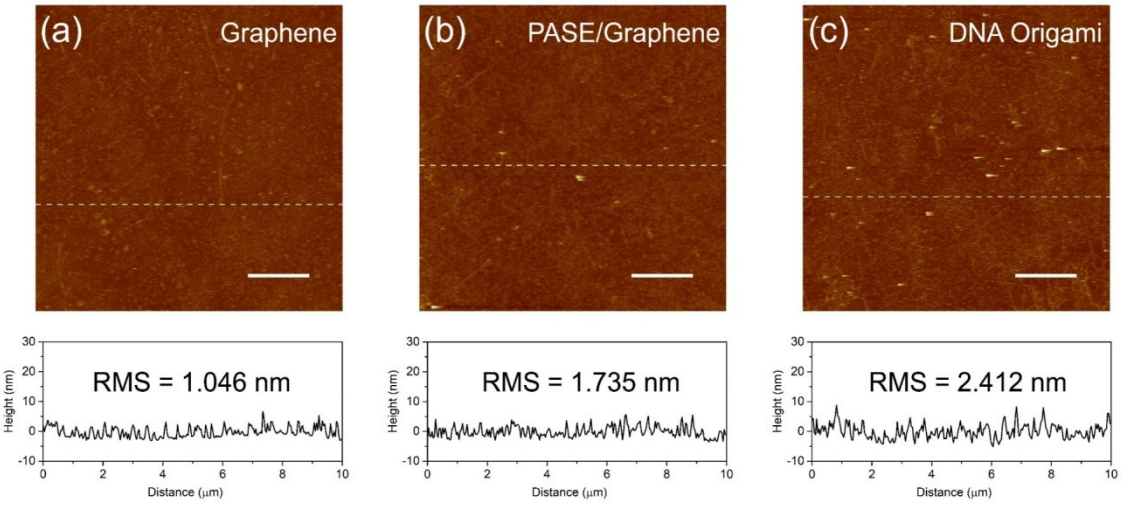

Fig. S7. AFM images of (a) pristine graphene, (b) PASE modified graphene and (c) DNA Origami modified graphene. Scale bars are 2 μm.

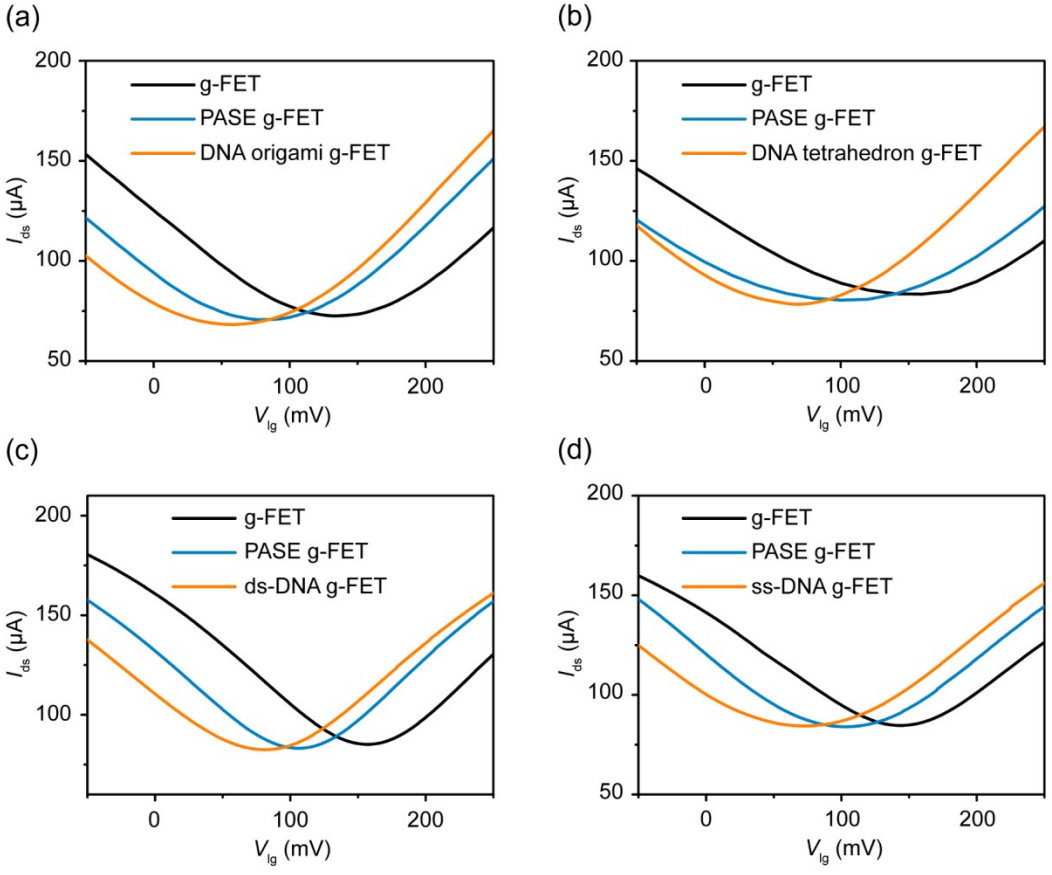

Fig. S8. Transfer curves of bare g-FET, PASE modified g-FET and DNA materials modified g-FET (V_{ds}= 50 mV). DNA materials are (a) DNA origami, (b) DNA tetrahedron (c) ds-DNA and (d) ss-DNA.

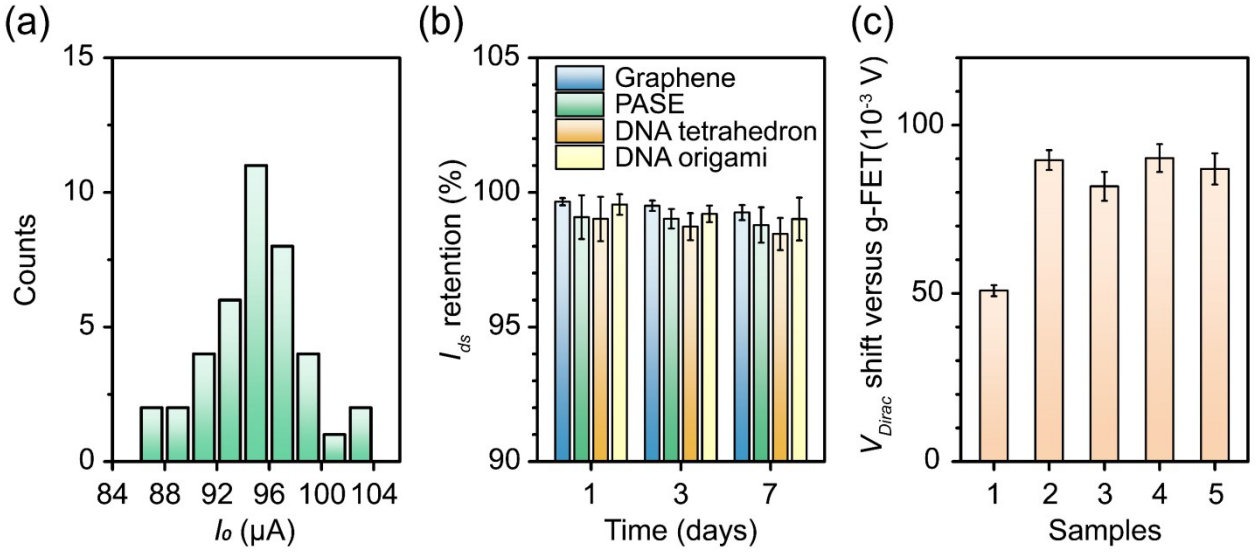

171

172 **Fig. S9.** (a) The I_0 distribution of DNA origami modified g-FETs before UVC irradiation (V_{ds}= 50 mV).
173 (b) I_{ds} retention of bare g-FETs, PASE modified g-FETs, DNA tetrahedron modified g-FETs and DNA
174 origami modified g-FETs. (c) The Dirac point shift versus bare g-FETs of the devices modified by PASE
175 and DNA materials. Sample 1–5: PASE, ss-DNA, ds-DNA, DNA tetrahedron and DNA origami.

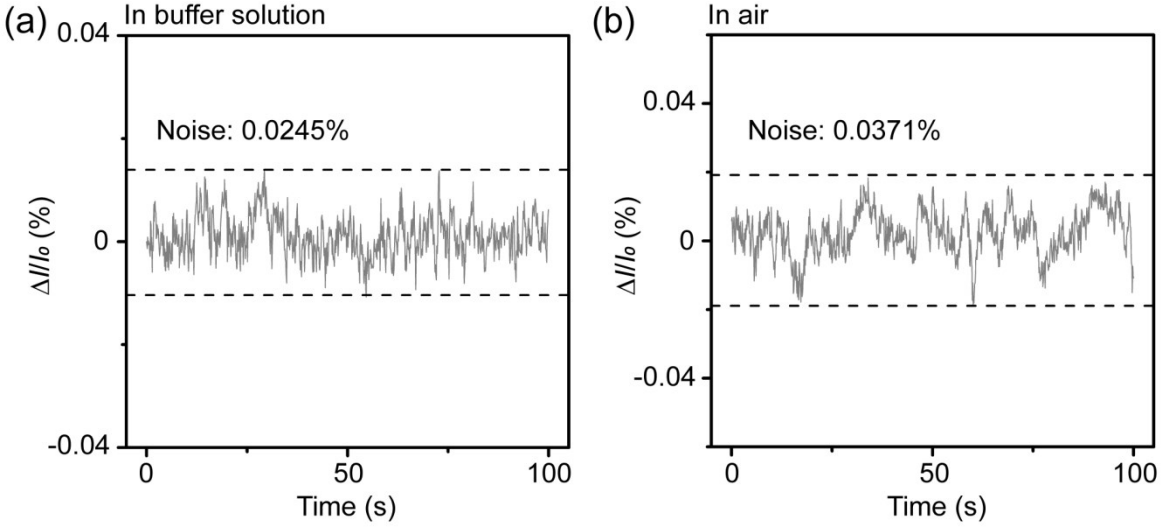

176

177 **Fig. S10.** Real-time $\Delta I/I_0$ response versus time of DNA origami modified g-FETs working in buffer
178 solution (a) and in air (b). The noises are measured to be 0.0245% and 0.0371%.

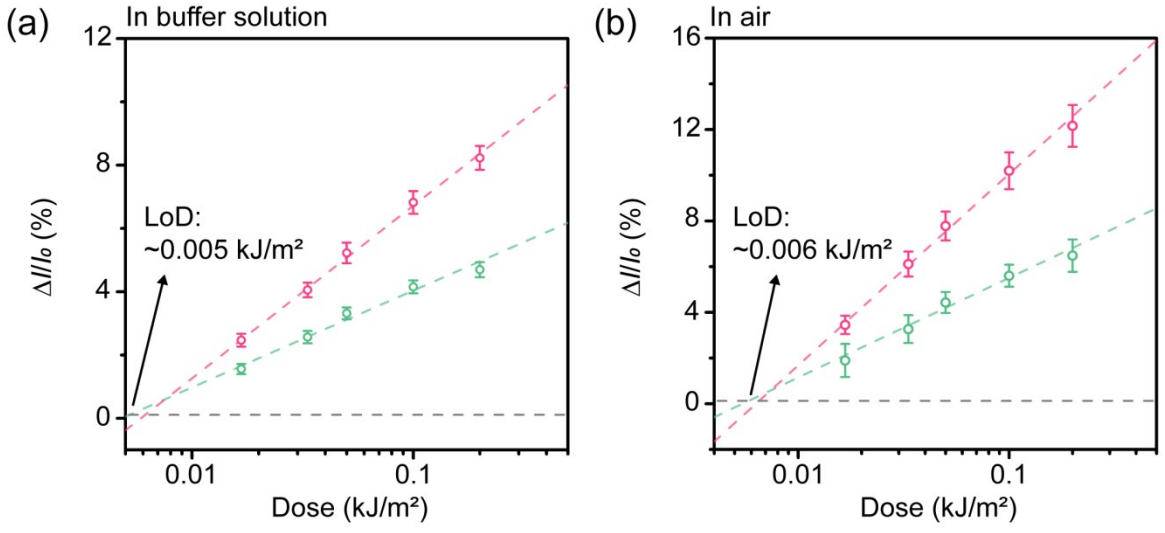

179

180 **Fig. S11.** $\Delta I/I_0$ versus UVC dose and LoD calculation of devices working in buffer solution (a) and in air
181 (b). Red data points and red dotted lines represent response of DNA origami modified g-FETs, green data
182 points and green dotted lines represent response of DNA tetrahedron modified g-FETs.

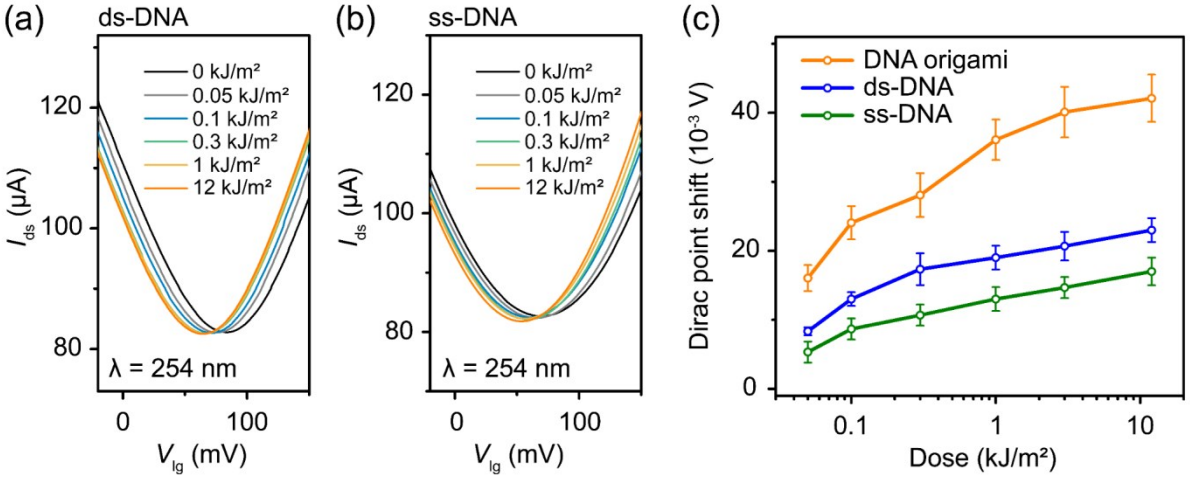

183

184 **Fig. S12.** (a) Transfer curves of the dosimeters modified with ds-DNA at different UVC doses (V_{ds}= 50
185 mV). (b) Transfer curves of the dosimeters modified with ss-DNA at different UVC dose (V_{ds}= 50 mV).
186 (c) The Dirac point shift versus doses of the UVC dosimeters modified with DNA origami, ds-DNA and
187 ss-DNA.

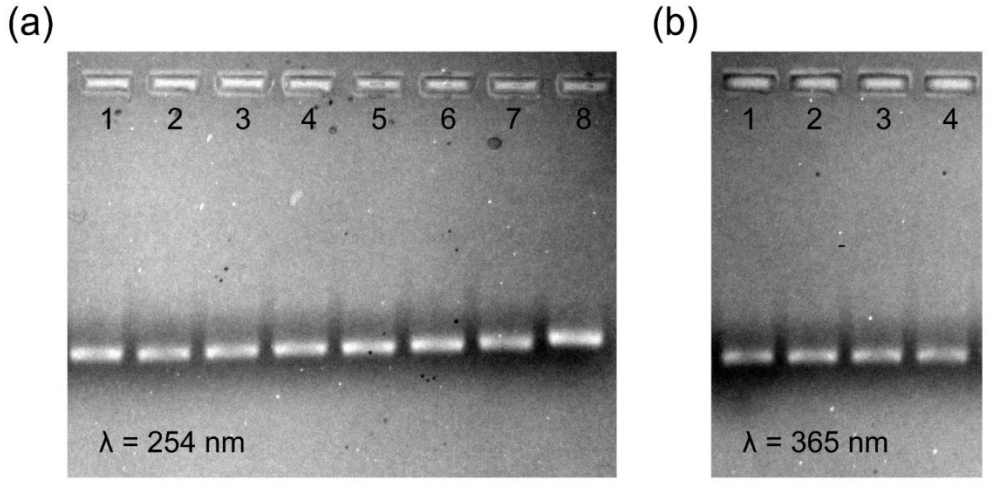

188

189 **Fig. S13.** (a) AGE characterizations of DNA origami at various UVC doses. Lanes 1–8: 0, 0.1, 0.3, 0.5,
190 1, 3, 6 and 12 kJ m^{-2} doses, respectively. (b) AGE characterizations of DNA origami at various UVA
191 doses. Lanes 1–4: 0, 10, 40 and 120 kJ m^{-2} doses, respectively.

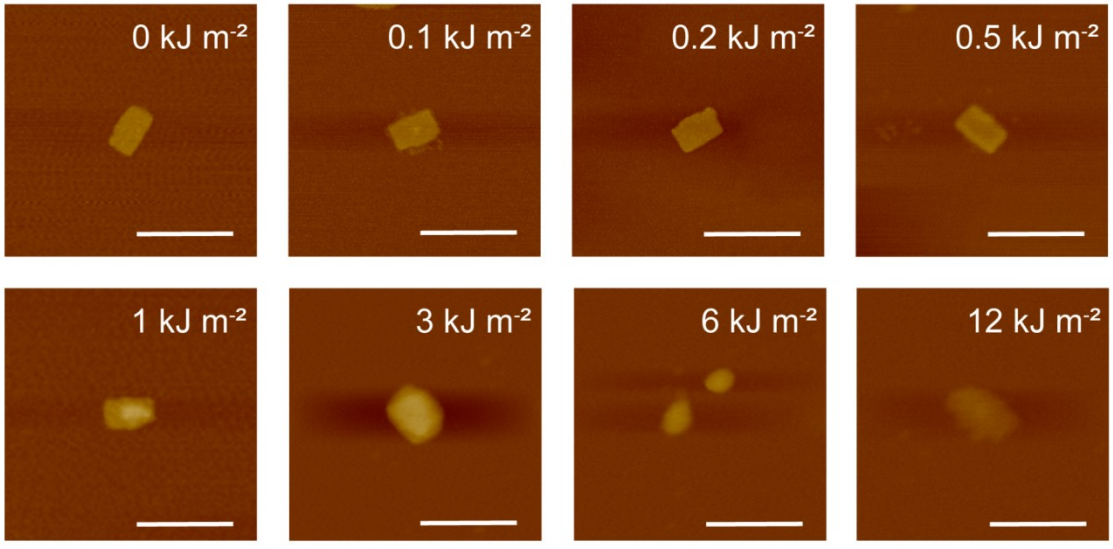

192

193 **Fig. S14.** AFM images of DNA origami at various UVC doses. Scale bars are 200 nm.

194

195

4 Supplementary Table

Materials	Methods	Target UV	Range (kJ m^{-2})	Highlights	Ref
The viologen-based polymer with an Anderson-like metal carboxylate cluster	Colorimetric method	UVA	6.72–17.42	Wide dynamic dose range and improving the repeatability of the photochromic process	6
(4-phenoxyphenyl) diphenylsulfonium triflate with crystal violet lactone and Congo red	Colorimetric method	UVA	0.5–8	Providing wearable, highly sensitive and accurate measurements	7
An ink consisting of a multi-redox polyoxometalate and an e^- donor	Colorimetric method	UVC	0.025–18	Low cost, highly sensitive and stable detection	8
Gel infused with leuco crystal viole, 4-(1,1,3,3-tetramethylbutyl) phenyl-polyethylene glycol and trichloroacetic acid	Colorimetric method	UVC	0.05–1.5	3D dosimeter with high sensitivity	9
Polycaprolactone doped with tetrazolium salts	Colorimetric method	UVC	0.5–20	Low uncertainty and wide dynamic dose range	10
DNA Origami	Agarose gel electrophoresis	UVC	4.25–34	First work to use UV radiation to control DNA origami conformation	11
DNA Origami	Atomic force microscope	UVC	2.16–25.92	New method to detect UV dose with high biocompatibility	12
DNA nanostructures	Transistor sensor	UVC	0.005–6	Rapid, portable, quantitative, highly sensitive, specific and easily operational detection of UVC dose	This work

Table S1. Sensing properties of some UV dosimeters and their highlights.

References

1. P. W. K. Rothemund, *Nature,* 2006, **440**, 297–302.

2. M. Lin, J. Wang, G. Zhou, J. Wang, N. Wu, J. Lu, J. Gao, X. Chen, J. Shi, X. Zuo and C. Fan, *Angew. Chem. Int. Ed.*, 2015, **54**, 2151–2155.

3. S. Xu, J. Zhan, B. Man, S. Jiang, W. Yue, S. Gao, C. Guo, H. Liu, Z. Li, J. Wang and Y. Zhou, *Nat. Commun.*, 2017, **8**, 14902.

4. Y. Ohno, K. Maehashi, Y. Yamashiro and K. Matsumoto, *Nano Lett.*, 2009, **9**, 3318–3322.

5. X. Guo, A. A. Gorodetsky, J. Hone, J. K. Barton and C. Nuckolls, *Nat. Nanotech.* 2008, **3**, 163–167.

6. S. Li, M. Han, Y. Zhang, G. Li, M. Li, G. He and X. Zhang, *J. Am. Chem. Soc.*, 2019, **141**, 12663–12672.

7. H. Araki, J. Kim, S. Zhang, A. Banks, K. E. Crawford, X. Sheng, P. Gutruf, Y. Shi, R. M. Pielak and J. A. Rogers, *Adv. Funct. Mater.*, 2017, **27**, 1604465.

8. W. Zou, A. Gonzalez, D. Jampaiah, R. Ramanathan, M. Taha, S. Walia, S. Sriram, M. Bhaskaran, J. M. Dominguez-Vera and V. Bansal, *Nat. Commun.*, 2018, **9**, 3743.

9. M. Kozicki, M. Bartosiak, M. Dudek and S. Kadlubowski, *J. Photoch. Photobio. A.*, 2021, **405**, 112930.

10. E. Sąsiadek and M. Kozicki, *Autex Res. J.*, 2020, **20**, 140–147.

11. H. Chen, R. Li, S. Li, J. Andreasson and J. Choi, *J. Am. Chem. Soc.*, 2017, **139**, 1380–1383.

12. W. Fang, M. Xie, X. Hou, X. Liu, X. Zuo, J. Chao, L. Wang, C. Fan, H. Liu and L. Wang, *J. Am. Chem. Soc.*, 2020, **142**, 8782–8789.